Measurement 163 (2020) 107995

Contents lists available at ScienceDirect

Measurement

journal homepage: www.elsevier.com/locate/measurement

Comparative analysis of real-time kinematic and PPP techniques in dynamic environment

Reha Metin Alkan [a], Serdar Erol [a,*], Veli İlçi [b], İ. Murat Ozulu [c]

[a] Department of Geomatics Engineering, Istanbul Technical University, Istanbul, Turkey
[b] Department of Geomatics Engineering, Ondokuz Mayıs University, Samsun, Turkey
[c] Department of Technical Programs, Hitit University, Çorum, Turkey

ARTICLE INFO

Article history:
Received 5 February 2020
Received in revised form 27 March 2020
Accepted 17 May 2020
Available online 26 May 2020

Keywords:
Kinematic positioning
Precise Point Positioning (PPP)
Real-time PPP
Single-baseline RTK
Network RTK

ABSTRACT

The main objective of this study is to assess the performance of the relative Real-time Kinematic (RTK) Global Navigation Satellite System (GNSS) Methods; i.e., Single-baseline & Network RTK, and Real-time Precise Point Positioning (RT-PPP); i.e., Trimble CenterPoint Real Time eXtended (RTX) Correction Service in a dynamic environment. For this purpose, a kinematic test was done within a vessel in Obruk Lake Dam in Çorum province, Turkey. The test area was situated in a deep valley and surrounded by high hills covered with dense trees. The real-time coordinates of each measurement epoch were simultaneously determined with Single-baseline RTK, Network RTK, and RTX RT-PPP methods by using three GNSS receivers. The real-time coordinates obtained from both RTK and RT-PPP methods were compared against the post-processed relative solution epoch-by-epoch. The results show that, the 3D position accuracies of real-time methods were found as ±6 cm, ±3 cm and ±7 cm for Single-baseline RTK, Network RTK and RT-PPP methods, respectively. This study demonstrates that although the Network RTK methods provided the best solution among the others, the positioning did not conduct most of the time due to the loss of cellular connection. This was also partially valid for the Single-baseline RTK method because the corrections from the base station via radio-link couldn't be received due to the rough terrain conditions. However, it was possible to make positioning with RTX Real-time PPP technique using satellite delivery GNSS products (corrections) continuously and in a robust manner within the cm-level accuracy. Our study showed that the use of the global multi-GNSS RTX correction service outcompetes conventional RTK methods with providing consistent, reliable, and seamless cm-level accurate positioning almost without any interruption especially in challenging marine environments with severe terrain obstructions.

1. Introduction

The most common way to obtain cm-level accuracy with satellite-based positioning both in post-processed or real-time is carrier phase-based relative positioning. When the post-processed approach is considered, it requires at least two GNSS receivers (at least one for reference station with known coordinates and one for rover) and GNSS software for processing the collected data. These procedures generally need time-consuming and labour field and office works.

In the mid-1990s, with the development of the differential method called Real-time Kinematic (RTK) or Single-baseline RTK, it has become an essential real-time positioning tool in surveying and many other applications for which high accuracy is required. In this method, a GNSS receiver is deployed as base (reference) station at a known coordinate and transmits the correction to rover receiver(s) with a UHF radio modem [12]. The necessity for at least two receivers and a communication link between reference and rover receivers increases the measurement costs and complicates the field studies. The RTK provides positioning accuracy from several centimetres up to 0.1 m in the vicinity of a base station. This method requires only a few seconds to a few minutes initialization time to fix the phase ambiguities. It should be noted that the distance between the reference station and its rover receivers is limited between 10 and 20 km to resolve the carrier phase ambiguities rapidly and reliably. This limitation is caused by distance-dependent errors such as orbital, ionospheric, and tropospheric errors [33]. In this method, the attainable RTK positioning accuracy decreases while increasing the distance from the base station. When this method is performed, it is not possible to receive the corrections after a certain distance from the reference station,

* Corresponding author.
E-mail addresses: alkanr@itu.edu.tr (R.M. Alkan), erol@itu.edu.tr (S. Erol), veli.ilci@omu.edu.tr (V. İlçi), imuratozulu@hitit.edu.tr (İ. Murat Ozulu).

https://doi.org/10.1016/j.measurement.2020.107995
0263-2241/

and after this distance, another base station(s) would be required. This issue negatively affects the productivity of the field study while increasing the operating costs especially in extensive areas or extended projects through a line like roads, railways, or pipelines[23]. Besides, getting correction via radio link connection under hilly terrain conditions and challenging environment can be a problem, even if the distance is short. With a long-range RTK approach using the internet connection, it is possible to make RTK positioning for a greater distance, i.e., 50 km and more baseline length [5,20].

To mitigate the distance-dependent errors, traditional Single-baseline RTK was extended to multi-baseline, Network RTK (NRTK), by adding real-time kinematic positioning ability to the Continuously Operating Reference Stations (CORS) network[38]. When compared to Single-baseline RTK, the distance-dependent errors in NRTK are modelled more accurately and reliably for long baselines, i.e., several tens of kilometres [34]. NRTK provides homogenous cm-level accuracy and improves the reliability of positioning over extended distances[11]. Thus, one of the most accurate RTK positioning methods with high reliability and productivity is NRTK, which uses corrections from a network of reference stations[35]. Although NRTK has several advantages, it also has some disadvantages, including increased costs for network installation and maintenance, more complex hardware and software need and robust communication requirements and so on [21]. Furthermore, cellular/internet coverage over the study area is essential to use for this method. The kinematic performance of the Network RTK has been investigated in scientific researches [28,42,40]and what was found is that the positioning could be conducted within cm-level accuracy in NRTK. It should be emphasised that this method required an internet connection via typically cellular networks in order to receive the corrections. If any loss of connection occurs from technical reasons or terrain conditions, this method will become unusable. In this case, users turn to new accurate and faster positioning techniques to fill the gaps that exist in conventional real-time relative positioning techniques [36]. This absolute GNSS method is called as Precise Point Positioning (PPP).

Over the last decades, it has been possible to achieve real-time positioning with the advent of the real-time GNSS precise satellite orbit, clock correction data, and code and phase biases with a single GNSS receiver. In April 2013, the International GNSS Service (IGS) as a main standard high-quality GNSS data and product provider, has launched an open-access the Real-time Service (RTS) for Real-time Precise Point Positioning (RT-PPP) applications [41]. The IGS RTS broadcasts the satellite orbit and clock correction streams to the users via open standard Networked Transport of Radio Technical Commission for Maritime Services (RTCM) via Internet Protocol (NTRIP). The availability of precise products emerges the RT-PPP wherever mobile communication is available. Although RTS is currently provided as a GPS-only operational service, the GLONASS is initially provided as an experimental product and will be fully in service when the IGS feels confident. Other GNSS constellations will be added to the service when they will be ready. The users can access the service through subscription as well NTRIP client application like Bundesamt für Kartographie und Geodäsie (BKG) (Federal Agency for Cartography and Geodesy) NTRIP Client (BNC), Real-time Kinematic Library (RTKLIB), and others ([43] URL 1). When the RT-PPP with IGS-RTS positioning is conducted, it is necessary to use a internet connected computer that have proper software installed in order to retrieve IGS products and GNSS observables [29]. It should be expressed that; the PPP technique requires long initialization time (typically 15–60 min) in order to converge to cm-level of accuracy and this would limit the usability of this technique in real-time applications. In addition, the lack of real-time PPP algorithms in all GNSS receivers limits the usability of PPP in real-time applications. Furthermore, the RT-PPP needs high-end dual/multiple-frequency GNSS receiver and the high price of this kind of receivers is a major limitation to its adoption by a wide range of applications [31]. In this case, NTRIP client applications could be used in order to access the real-time data streams delivered by the IGS RTS or similar services. In case of a sudden communication interruption (internet loss), a discontinuity in receiving real-time IGS products occurs. Such a situation, which can be commonly occurred in the field conditions, restricts or limits the use of this method especially in the kinematic applications. It should be noted that the IGS doesn't guarantee the accuracy or availability of the Real-time Service [19].

Many studies in literature processed the IGS station data epoch by epoch (as pseudo-kinematic session) while applying RT-PPP method using IGS-RTS products. Elsobeiey and Al-Harbi [16] is an example of these kind of studies. Beside of these studies, in a number of publications, which based on the kinematic experimental investigations, RT-PPP method has been applied through real kinematic scenario. Monico et al. [29] and Yang et al. [41] are examples of the later. These studies showed that the most significant drawbacks of the RT-PPP were found as the relatively long initialization time and low accuracy, within a couple of decimetres to even sub-meter.

More recently, as an alternative to RTK techniques, commercial satellite or internet-based GNSS RT-PPP correction services have become available and have been used for highly accurate positioning in a wide range of applications including survey&mapping, seismology, agriculture, mining, oil&gas, railways, monitoring of civil engineering constructions, navigation, precise positioning for autonomous vehicle driving system, and so on. Nowadays, there are numerous satellite and/or internet-based global correction services such as Trimble RTX by Trimble Inc., Starfix by Fugro, StarFire by NavCom Technology Inc., Apex by Veripos (Hexagon), TerraStar by NovAtel (Hexagon), Atlas by Hemisphere GNSS Inc., and they are increasing day by day [3,27]. The products and necessary corrections are generally computed from the service's network consisting of GNSS reference stations, spread across the globe and the correction signals are delivered via L-band geostationary satellites or over the internet at accuracies ranging from sub-meter to centimetre-levels. Such services eliminate some of the drawbacks in both Single-baseline and Network RTK and conventional PPP techniques while combining their advantages in a modern technique. The services provide centimetre-level high accurate multi-GNSS positioning in real-time globally with only using a single receiver within relatively short convergence time.

This study aims to evaluate the performance of the carrier-phase-based Real-time Kinematic GNSS methods, considering both conventional Single-baseline RTK and Network RTK methods, and RTX real-time PPP global correction service in a dam lake situated in a deep valley and surrounded by high hills covered with dense trees. For this purpose, a realistic kinematic test that lasted about 6 h was conducted. Through the test, it was not possible to use fully either of the methods, Single-baseline and Network RTK, without any interruption due to study area conditions. In this study, the usability of satellite-based real-time PPP as an alternative to the conventional RTK methods in a harsh environment has been tested.

2. Theoretical background of the applied methods

2.1. Single-baseline RTK method

In order to understand positioning with RTK, it is necessary to remember some concepts and observation equations related to differential positioning. The conventional GNSS pseudo-range and carrier-phase observation equations between the satellite $\boldsymbol{s}$ (i and

j) and the receiver $\boldsymbol{r}$ (A, base receiver and B, rover receiver) are given as [22,10],

$$R_r^s(t) = \rho_r^s(t) + cdT_r(t) - cdt^s(t) + I_r^s(t) + T_r^s(t) + M_r^s(t) + E_r^s(t) + \varepsilon_r^s(t) \quad (1)$$

$$\Phi_r^s(t) = \rho_r^s(t) + cdT_r(t) - cdt^s(t) - I_r^s(t) + T_r^s(t) + M_r^s(t) + E_r^s(t) + \lambda N_r^s + \varepsilon_r^s(t) \quad (2)$$

where

R_r^s and Φ_r^s are the pseudorange and carrier-phase measurements between the satellite $\boldsymbol{s}$ and the receiver $\boldsymbol{r}$, respectively,
ρ_r^s is the geometric range between the satellite $\boldsymbol{s}$ and the receiver $\boldsymbol{r}$ (m),
dT_r is the receiver clock error (second),
dt^s is the satellite clock error (second),
I_r^s is the ionospheric delay error (m),
T_r^s is the tropospheric delay error (m),
M_r^s is the multipath error (m),
E_r^s is the orbital error (m),
N_r^s is the carrier phase integer ambiguity,
ε_r^s is the random errors (m).

The Pseudorange Correction (*PRC*) and Carrier-Phase Correction (*CPC*) at the known base station receiver (A) with the help of the satellites $\boldsymbol{s}$ are calculated. These differential corrections can be expressed in the following equations with ignoring the multipath error and random errors;

$$PRC_A^s(t) = \rho_A^s(t) - R_A^s(t) = -cdT_A(t) + cdt^s(t) - I_A^s(t) - T_A^s(t) - E_A^s(t) \quad (3)$$

$$CPC_A^s(t) = \rho_A^s(t) - \Phi_A^s(t) = -cdT_A(t) + cdt^s(t) + I_A^s(t) - T_A^s(t) - E_A^s(t) - \lambda N_A^s \quad (4)$$

These corrections are then broadcasted to the rover receiver (B) and the corrected pseudorange and carrier-phase observations are calculated with the equations:

$$R_B^s(t)_{corrected} = R_B^s(t) + PRC_A^s(t) = \rho_B^s(t) + cdT_{AB}(t) + \Delta I_{AB}^s(t) + \Delta T_{AB}^s(t) + \Delta E_{AB}^s(t) \quad (5)$$

$$\Phi_B^s(t)_{corrected} = \Phi_B^s(t) + CPC_A^s(t) = \rho_B^s(t) + cdT_{AB}(t) - \Delta I_{AB}^s(t) + \Delta T_{AB}^s(t) + \Delta E_{AB}^s(t) + \lambda N_{AB}^s \quad (6)$$

In the limited distance (less than 10 km) between reference (A) and rover (B), distance-dependent errors are highly correlated and can be neglected. In this case, the corrected pseudorange and carrier-phase observations for the rover (B) with the satellites i and j become;

$$R_B^i(t)_{corrected} = \rho_B^i(t) + c[dT_B(t) - dT_A(t)] \quad (7)$$

$$\Phi_B^i(t)_{corrected} = \rho_B^i(t) + c[dT_B(t) - dT_A(t)] + \lambda(N_B^i - N_A^i) \quad (8)$$

$$R_B^j(t)_{corrected} = \rho_B^j(t) + c[dT_B(t) - dT_A(t)] \quad (9)$$

$$\Phi_B^j(t)_{corrected} = \rho_B^j(t) + c[dT_B(t) - dT_A(t)] + \lambda(N_B^j - N_A^j) \quad (10)$$

By the differencing the corrected observations (Eqs. (7)–(10)) for the rover (B), the receiver clock errors are eliminated. Then the rover calculates its position in cm level with the corrected observations in real time, if the ambiguity resolution is fixed. Many ambiguity resolution methods are available in the literature, but the on-the-fly (OTF) technique is the most used one in real time positioning. The OTF ambiguity solution uses the wide-lane combination to resolve integer ambiguities and then use the resulting position to directly compute the ambiguities on the original carrier phase data [22,4].

Over limited distance, the errors in Single-baseline RTK increase and cannot be neglected. The atmospheric errors are spatially correlated and can be spatially modelled. In this case, Network RTK should be used.

2.2. Network RTK method

In order to mitigate the distance-dependent errors more accurately and reliably, Network RTK (NRTK) has started to be used within the last decades. In principle, the NRTK performs the following items in sequence[15]:

(i) Data are collected at the reference stations and transmit their data to a control centre in real-time,
(ii) With the known coordinate of reference stations, a network baseline solution between the reference stations carried out in the control centre. As a result, the phase ambiguities, the common clock errors and atmospheric delays are estimated for the network stations, and corrections are generated at the network processing (control) centre in real-time,
(iii) Then the interpolated corrections are broadcasted and the real-time position is determined at the rover.

Different from the Single-baseline RTK, the common phase ambiguities of the reference network and the common clock errors are considered as known in NRTK. In this case the *PRC* and *CPC* at the reference station receiver (A) are calculated as;

$$PRC_A^s(t) = \rho_A^s(t) + cdT_A(t) - cdt^s(t) - R_A^s(t) = -I_A^s(t) - T_A^s(t) - E_A^s(t) \quad (11)$$

$$CPC_A^s(t) = \rho_A^s(t) + cdT_A(t) - cdt^s(t) + \lambda N_A^s - \Phi_A^s(t) = +I_A^s(t) - T_A^s(t) - E_A^s(t) \quad (12)$$

Then, the corrected observations for the rover receiver (B) are created as:

$$R_B^s(t)_{corrected} = \rho_B^s(t) + cdT_B(t) + \Delta I_{AB}^s(t) + \Delta T_{AB}^s(t) + \Delta E_{AB}^s(t) \quad (13)$$

$$\Phi_B^s(t)_{corrected} = \rho_B^s(t) + cdT_B(t) - \Delta I_{AB}^s(t) + \Delta T_{AB}^s(t) + \Delta E_{AB}^s(t) + \lambda N_B^s \quad (14)$$

The distance dependent errors estimated at the control centre are spatially highly correlated and can be interpolated for the position of the various rover receivers in different correction methods. In NRTK system, many correction methods can be used, including Flächen-Korrektur Parameter (FKP), Virtual Reference Station (VRS), Master-Auxiliary Concept (MAC), Individualized Master-Auxiliary Corrections (iMAX), and Pseudo Reference Station (PRS).

The FKP method allow the interpolation of the distance dependent errors (DDE) for the approximate position of the rover receiver (B) from the reference receiver (A) as[39]:

$$\Delta DDE_{AB}^s = f(FKP_A^s, \Delta\varphi_{AB}, \Delta\lambda_{AB}, \Delta h_{AB}) \quad (15)$$

The VRS method can be computed from FKP method easily, because all necessary information is included in the data stream to interpolate the corrections for a given rover position. The rover has to send its approximate position to the network, which then interpolates from the state information a reference data stream $\boldsymbol{VRS_{AB}^s}$ for the given position as follow [39]:

$$VRS^{s}_{AB} = \Phi^{s}_{B}(t)_{corrected} + \Delta DDE^{s}_{AB} \quad (16)$$

Finally the rover user can achieve cm-level position accuracy by applying the differential corrections provided by the network while the fixing of the phase ambiguities [10].

In Turkey, like in the world, a multi-baseline RTK network that is called TUSAGA-Aktif (or Turkish RTK CORS Network/CORS-TR) was established and has been serving to positioning community since 2009. This network, covering almost all of Turkey and the Turkish Republic of Northern Cyprus, comprises 146 reference stations and two control stations (Master and Auxiliary). The average distance between the stations is 70 to 100 km in length. The two control centres of TUSAGA-Aktif are located in Ankara, the capital city of Turkey. By virtue of several advantages of the system, it has been widely used in many different positioning applications across Turkey. TUSAGA-Aktif uses the VRS, FKP, and MAC and Differential GPS (DGPS) techniques. The control centres of the TUSAGA-Aktif Network have been continuously logged the RINEX data daily 1- and 30-second interval from the reference station for later use.

2.3. Trimble RTX real-time PPP service

In this study, one of the satellite-based GNSS correction services, Trimble Real Time eXtended (RTX), was used. The Trimble RTX represents a family of GNSS correction services offering a variety of services with different accuracies as CenterPoint RTX, FieldPoint RTX, RangePoint RTX, and ViewPoint RTX. Within this study, only Trimble CenterPoint RTX was used, and that's why the information given in this section will be only about this service. The expression of "RTX" is used to mean "Trimble CenterPoint RTX Service" within this paper. RTX is a RT-PPP positioning service that was introduced in 2011 [25]. It is enabling cm-level real-time ambiguity-fixing precise absolute positioning service almost all over the world without the need of any reference station infrastructure. In this system, RTX products and corrections, precise satellite orbits, clock offsets, code and phase biases, and other auxiliary information, calculated with the help of approximately 120 globally distributed Trimble multi-GNSS reference stations. The generated products and corrections are then transmitted via the Trimble compressed data format CMRx to the user in real-time using L-band signals via a set of geostationary satellites or over the internet (e.g., thought a cellular data connection). The rover receiver combines the RTX corrections with its GNSS observations in order to produce accurate real-time positions [36]. The ionospheric effect is eliminated by using ionosphere-free combination of observations on L1 and L2 frequencies. The tropospheric delay is modelled plus additional unknowns for the vertical wet delay and two gradients in north-south and east-west direction [18]. It should be noted that, the receiver clock error is estimated in the rover user and the receiver biases are obtained by combining the divergence-free phase combination and the code measurement [25]. The schematic depiction of RTX workflow is given in Fig. 1.

Trimble CenterPoint RTX offers extremely fast and precise GNSS corrections for PPP solutions. RTX global correction service initially supported the GPS and GLONASS satellites, today it provides correction data for all available GNSS constellations including GPS, GLONASS, Galileo, BeiDou and QZSS satellites [6]. The system eliminates the need for a cellular coverage or internet connection, which is a problem in Single-baseline or Network RTK techniques, and supports getting correction from L-band geostationary satellites with capable antennas and receivers.

The Trimble RTX family provides accuracies ranging from submeter to centimetre-level depending on chosen RTX services. Among them, the CenterPoint RTX service provides 2 cm horizontal and 5 cm vertical accuracy (RMS). It is worth mentioning that, on the dates of this study, the RTX delivered a 4 cm horizontal accuracy (till August 6th, 2018). The final coordinates were given in ITRF2008 datum 2005.00 epoch before March 23rd, 2017. Thereafter, the corrected coordinates are derived in the observation (cur-

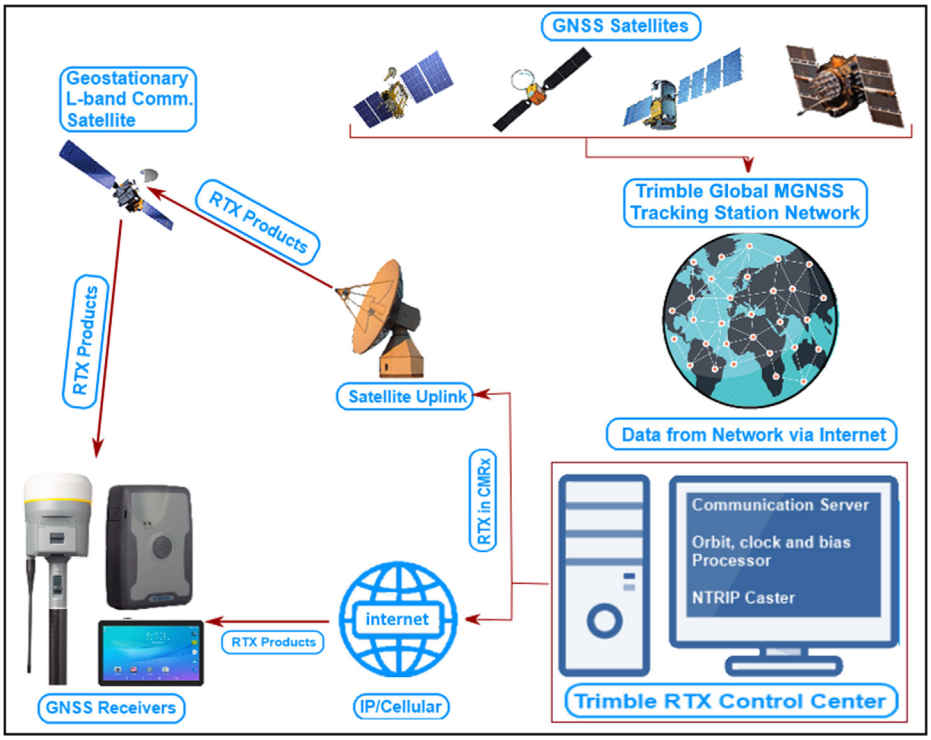

Fig. 1. The schematic depiction of RTX workflow.

rent) epoch of ITRF2014, and these coordinates are transformed into ITRF2014 datum 2005.00 epoch ([44] URL 2) with the help of MORVEL56 Plate Motion Model (PMM).

Additionally, global ionospheric and/or regional ionospheric and tropospheric corrections are also computed in RTX system, which are then applied to help reduce the time of convergence in RTX positioning. The global ionosphere model (GIM) was first used in RTX system to further reduce the convergence time in 2013. In addition, regional atmospheric (ionospheric and tropospheric) models started to be used in Trimble RTX Fast Regions in 2015 for very fast convergence [30]. In these solutions, the ionospheric delays are constrained to resolve ambiguities that uses narrow-lane code and wide-lane phase combination to get the wide-lane ambiguities [17]. In normal conditions, the RTX convergence time for specified precisions is 15 min or less in the worldwide while being less than 1 min in the selected regions (Trimble RTX Fast Regions). The CenterPoint RTX QuickStart and CenterPoint RTX Fast Restart features provide fast initialization within less than 1 min if the measurement is started on a point with known coordinates, or used in the same place that it was the last turned-off. When comparing the RTX to the conventional PPP technique with respect to the convergence time issue, it is obvious that RTX has a significant advantage.

Although the service has several advantages, it also has some drawbacks. One of them is that the users require a receiver with PPP firmware and antenna capable of receiving Trimble RTX products and corrections. It also requires a subscription to the service.

The performance of RTX service has been studied by researchers within a limited number of studies. Chen et al. [8], who carried out one of the first studies on this subject, tested the RTX system performance and they found that the RTX was superior to conventional Network RTK concept in terms of final accuracy in static and kinematic modes. As one of the first studies, the RTX was investigated in terms of accuracy on land, and they found that it is possible to make positioning cm-level of accuracy worldwide in real-time in static and kinematic modes with RTK productivity [25]. Carballido et al. [7] investigated the usability of RTK and RTX (from satellite) on the autonomous vehicle developed for agriculture applications. The results of their study show that the RTX could be used on an autonomous tractor while reducing the equipment cost. Ochałek et al. [32] investigated the accuracy verification of the Trimble RTX in a static measurement. They concluded that the RTX meets the accuracy requirements given by the Trimble. The RTX technique was used for precise agricultural operations on a peanut crop, and very promising results were obtained [13]. The performance of the RTX in a kinematic application was investigated by Alkan [1]. The results imply that it was possible to make cm-accurate positioning. Ilci [24] investigated the positioning performance and convergence time of the RTX and compared to both Single-baseline and Network RTK in a static application.

The Trimble CenterPoint RTX technology was discussed more intensively with technical details and the methodology by Leandro et al. [25], Leandro et al. [26], Doucet et al. [14], Chen at al. [9], Talbot et al. [37], Richter [36], [44] URL 2.

The basic code and phase measurement equations for the PPP solution of rover B are given as follows [2]:

$$R^S_{Bi} = \rho^S_B + c\left(dT_B - dt^S\right) + T^S_B + I^S_B + A_i - a_i + B_{R_i} - b_{R_i} + D + Rel + M_{R_i} + \varepsilon_{R_i} \quad (17)$$

$$\Phi^S_{Bi} = \rho^S_B + c\left(dT_B - dt^S\right) + T^S_B - I^S_B + \lambda_i N^S_B + A_i - a_i + (W_\Phi - w_\Phi)\lambda_i + B_{\Phi_i} - b_{\Phi_i} + D + Rel + M_{\Phi_i} + \varepsilon_{\Phi_i} \quad (18)$$

$A_i$and a_i: receiver and satellite antenna offsets for ith frequency (m), respectively,
W_Φ and w_Φ: receiver and satellite antenna phase wind-up effect (cycles), respectively,
B_{Φ_i} and b_{Φ_i}: carrier-phase receiver and satellite bias for ith frequency (m), respectively,
B_{R_i} and b_{R_i}: pseudorange receiver and satellite bias for ith frequency (m), respectively,
M_{Φ_i} and M_{R_i}: carrier-phase and pseudorange multipath for ith frequency (m), respectively,
ε_{Φ_i} and ε_{R_i}: carrier-phase and pseudorange observation noise and other un-modelled effects for ith frequency (m), respectively,
D: combined site displacement effects due to earth, ocean tide and atmospheric loading (m),
Rel: relativistic effects (m),

In order to remove the first-order ionospheric effect, the following ionosphere-free (IF) equations are used[2]:

$$\Phi_{IF} = (f_1^2.\Phi_1 - f_2^2.\Phi_2)/(f_1^2 - f_2^2) \quad (19)$$

$$R_{IF} = (f_1^2.R_1 - f_2^2.R_2)/(f_1^2 - f_2^2) \quad (20)$$

In these equations, $\Phi_{IF}$and R_{IF} are the ionosphere-free carrier-phase and pseudo-range measurements (m), respectively, and, f_1 and f_2 are the carrier-phase frequencies (Hz).

In order to achieve high-accurate position with this absolute positioning technique PPP, the additional corrections like phase wind-up effect, satellite/receiver antenna phase centre offset and variations, site displacement effects including solid earth, ocean tide and atmospheric loading, sagnac effect, relativistic effect, code and carrier-phase biases, and others should be applied[31].

3. Kinematic test

In this study, the performance of the three different methods, i.e., Single-baseline RTK, Network RTK, and RTX RT-PPP, were investigated in a dynamic environment. Within this frame, a kinematic test was carried out in Obruk Lake Dam in June of 2017. Obruk Dam was built on Kızılırmak River in Çorum province, Turkey, to produce irrigation, drinking water, and energy. It has been operational since 2009. The water surface area is about 52.2 km^2, and the average elevation of the dam is about 460 m above the sea level (in front of the crest). Looking at the region from the point of surveying conditions, it is seen that the part of the water environment is located in deep valleys, and the water body is surrounded by high hills (approximately 1250 m height above sea level) covered with dense trees. In this context, it can be said that the study area has very harsh and challenging environmental conditions.

Before starting the kinematic test measurement, a local base (reference) station was established on the shore in the vicinity of the test area at a secure location for Single-baseline RTK. The coordinates of this point were calculated with respect to nearest TUSAGA-Aktif reference stations with the conventional post-processed relative method. The location of this point was selected to provide the maximum performance as clear as possible of obstructions and a clear line of sight to the sky for all possible satellites covering the maximum job site. After the receiver was set up at this base station, corrections were then started to be sent to the roving receiver with a radio link.

After the fully initialized, i.e., RTKs and CenterPoint RTX converges to cm-level of accuracy, the kinematic measurement was carried out along several survey profiles lasting 6 h by tracking all available satellite constellations at 1-second measurement

interval. In the study, a 12.5 m long and 3.5 m wide wooden leisure vessel was used. The total measurement length was about 56.1 km, and the vessel sailed through the measurement within an average speed of about 9.4 km/h (Fig. 2).

Data was collected with GNSS receivers on the locations that can be seen in Fig. 3 in the following configurations:

- **GNSS-1:** Receive RTX corrections via satellite and log the raw data for later processing at the 1-second interval,
- **GNSS-2:** Receive Network RTK corrections from TUSAGA-Aktif Turkish National CORS Network and log the raw data for later processing at the 1-second interval,
- **GNSS-3:** Receive Single-baseline RTK corrections and log the raw data for later processing at the 1-second interval.

It is worth mentioning that to be able to compare the methods with each other in terms of performance and accuracy, it was necessary to conduct the kinematic test with all three antennas under the same conditions as possible. However, it was not technically possible to perform all measurements with a single receiver at the same time. On the other hand, it was not possible to connect three different receivers to a single antenna via an antenna splitter, since the used receivers had an internal antenna. Because of these technical restrictions, all three antennas were mounted as close as possible to each other (a few meters away) on the vessel, and measurements were made simultaneously. In this way, all GNSS data were retrieved/collected by the all geodetic-grade GNSS receivers almost under the same surveying conditions, which allows for precise assessment of the handled three different GNSS measurement methods.

For all measurements, multi-constellation and multi-frequency Trimble R10 geodetic grade GNSS receiver with an internal antenna was used. The Trimble R10 receiver can track the GPS, GLONASS, Galileo, BeiDou, QZSS, and NavIC (IRNSS) satellite signals and L-band communications. The receiver is capable of positioning rates at 1 Hz, 2 Hz, 5 Hz, 10 Hz, and 20 Hz interval. Further specifications and detailed information can be found in ([45] URL 3).

Single-baseline RTK Measurement: The transmitted correction via radio link from the Local Base Station was retrieved with the GNSS-3 receiver. After initialization, the real-time coordinates of each measurement epoch were obtained. The distance between the vessel and the base point was found about 72 m to 5.3 km.

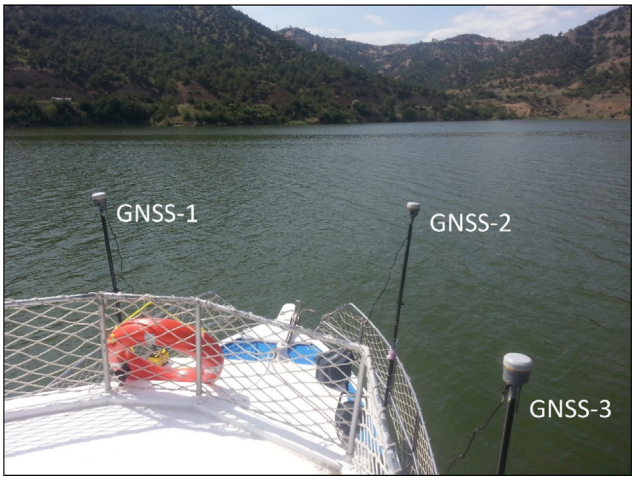

Fig. 3. The location of GNSS receivers in the surveying vessel used in this study.

Network RTK Measurement: The GNSS-2 receiver was connected to TUSAGA-Aktif CORS service via GSM connection and the corrections started to be received. After a few seconds initialization time, 3D coordinates of each measurement epoch were determined in real-time with the VRS correction technique.

Positioning with Trimble CenterPoint RTX Correction Service: At the beginning of the measurement, the GNSS-1 receiver was configured to receive CenterPoint RTX corrections via satellite. The used GNSS receiver, Trimble R10, is capable of tracking CenterPoint RTX correction service via satellite delivery or IP/cellular. After the R10 receiver was started to receive the RTX correction stream, the real-time coordinates of each measurement epoch were determined by tracking the CenterPoint RTX correction service using L-band geostationary satellite delivery.

The Trimble RTX correction service computes the real-time coordinates in the current epoch, and they will be transformed to ITRF2008 2005.00 epoch by using the selected tectonic plate's motion model embedded in its firmware. Thus, the accuracy of

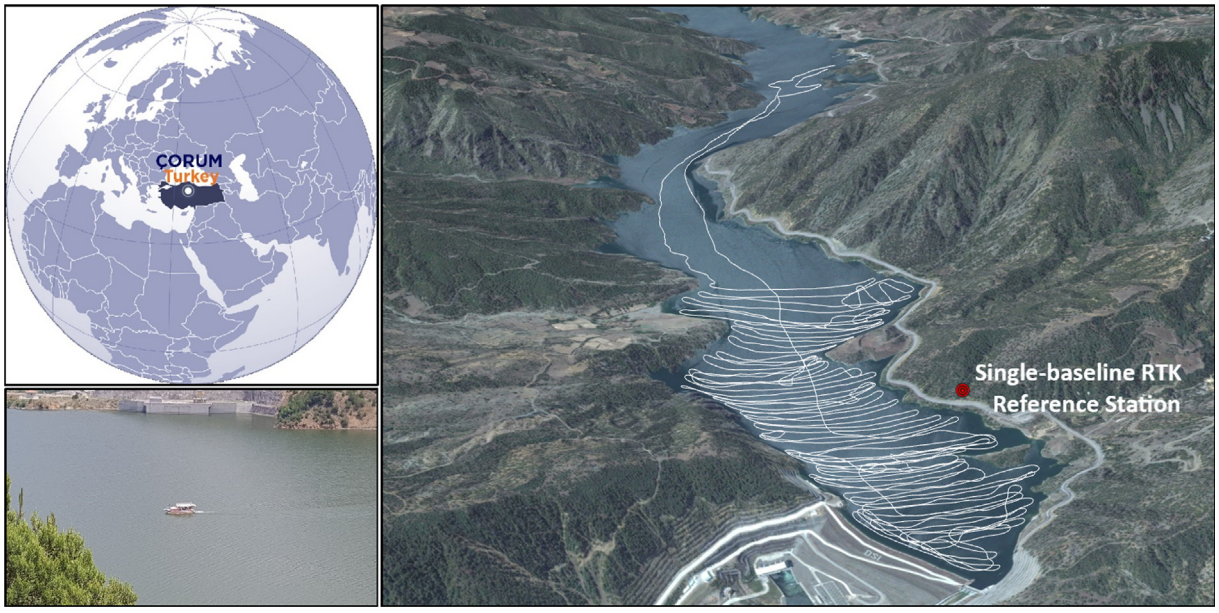

Fig. 2. The test area and vessel trajectory on google earth.

the resultant coordinates is closely influenced by the selected tectonic plate model. To obtain accurate results declared by the service provider, the proper tectonic plate should be selected (or introduced) at the beginning of the survey. It is considered that it would be very beneficial to clarify this issue before starting the measurements, especially in the regions where measurement is performed for the first time.

4. The evaluation of the collected data processing

In order to make a precise assessment of the handled methods (i.e. Single-baseline & Network RTK, and RTX), it was necessary to calculate the reference (known) coordinates of each epoch for three GNSS antennas. For this purpose, the raw data were recorded into the receivers' internal memory through the real-time measurements on the vessel. The reference coordinates of each three antennas at each measurement epoch were then calculated by post-processing of the collected GNSS data on the vessel and nearest TUSAGA-Aktif reference stations with the carrier phase-based relative method. For this study, necessary data with 1-second interval were taken from the service provider. All GNSS data were processed with GrafNav GNSS Post-Processing Software, and the known coordinates of each measurement epoch were calculated with an average of 25 mm standard deviation in height component and 15 mm standard deviation in horizontal component. In this way, the known coordinates of each measurement epoch were determined very accurately for all antennas, and this allows precise assessment of the used methods. In order to give an idea about the ionospheric and tropospheric condition during the kinematic test, the Zenith Tropospheric Delay (ZTD) and Vertical Total Electron Content (VTEC) values at rover receiver were calculated. It was found that, the ZTD varies depends on the time and has a value of between 2.243 m and 2.323 m. Concerning to VTEC value, it varied between 15.02 TECu and 16.75 TECu. The GrafNav Software is a powerful, high-precision, multi-GNSS (GPS, GLONASS, BeiDou, Galileo, and QZSS) data processing software developed by NovAtel Inc. It processes the data collected in static or kinematic mode with Relative and Precise Point Positioning (PPP) processing strategies. More detailed information for GrafNav can be found in ([46] URL 4).

Fig. 4 shows the processing steps, which were followed in this study.

The real-time coordinates obtained from the applied three methods were compared with those of the relative solution epoch by epoch. The differences in northing (n), easting (e), horizontal (2D) and ellipsoidal heights (h) are given in Fig. 5, Fig. 6, and Fig. 7, for the Single-baseline RTK, Network RTK, and RTX, respectively. It should be noted that, all coordinates must be transformed into the same plate model, datum and epoch of reference coordinates before comparison.

The gaps in the Fig. 5 and Fig. 6 meant that there were no real-time solutions through these measurement intervals. For Single-baseline RTK (Fig. 5), the solution didn't obtain because the corrections from the base station via radio-link couldn't be received. Concerning the Network RTK (Fig. 6), the positioning didn't conduct most of the time due to the loss of cellular internet connection.

To illustrate the frequency (distribution) of the calculated differences given in Figs. 5, 6 and 7, histograms were created and given in Fig. 8. The mean values and outliers that exist in the data set can also be identified via the corresponding histogram.

As can be seen in Fig. 8, the differences for Network RTK method was found within a few cm for 2D position while between −10 cm and 10 cm for height component (Fig. 8, *middle*). When the distribution of the differences of the other two methods (i.e., Single-baseline RTK and Trimble CenterPoint RTX) in histograms were examined (Fig. 8, *top* and *bottom*), it was seen that there are 'means' and 'outliers'. If the differences more than 2σ (95% confidence level) were excluded from the data set, it was found that the differences were fallen within the range of approximately −5

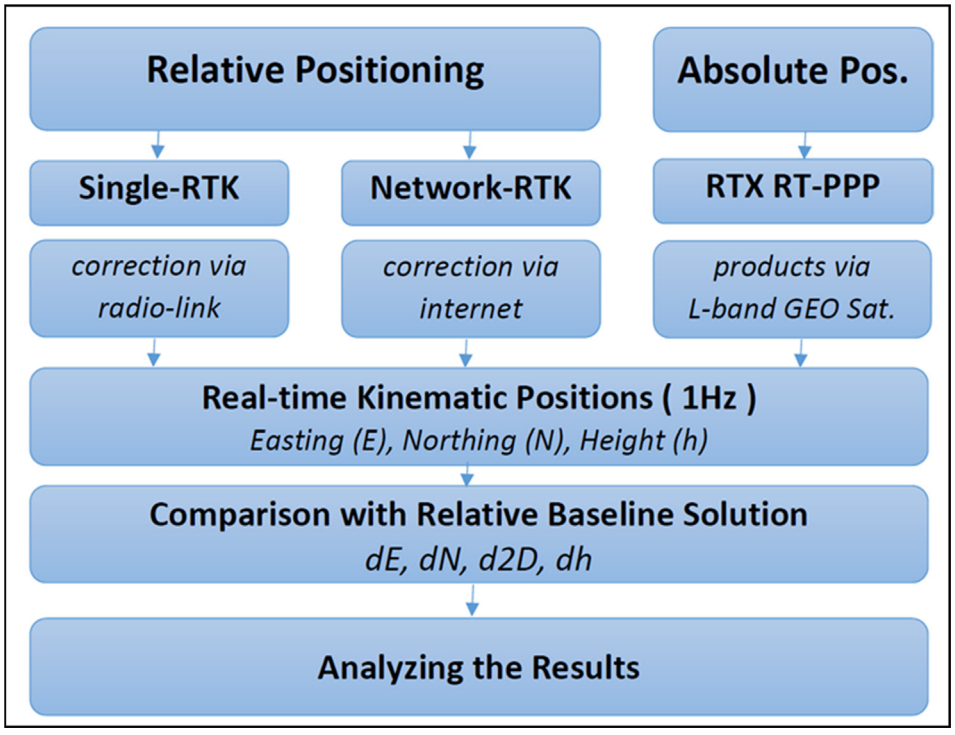

Fig. 4. Flowchart for research methodology.

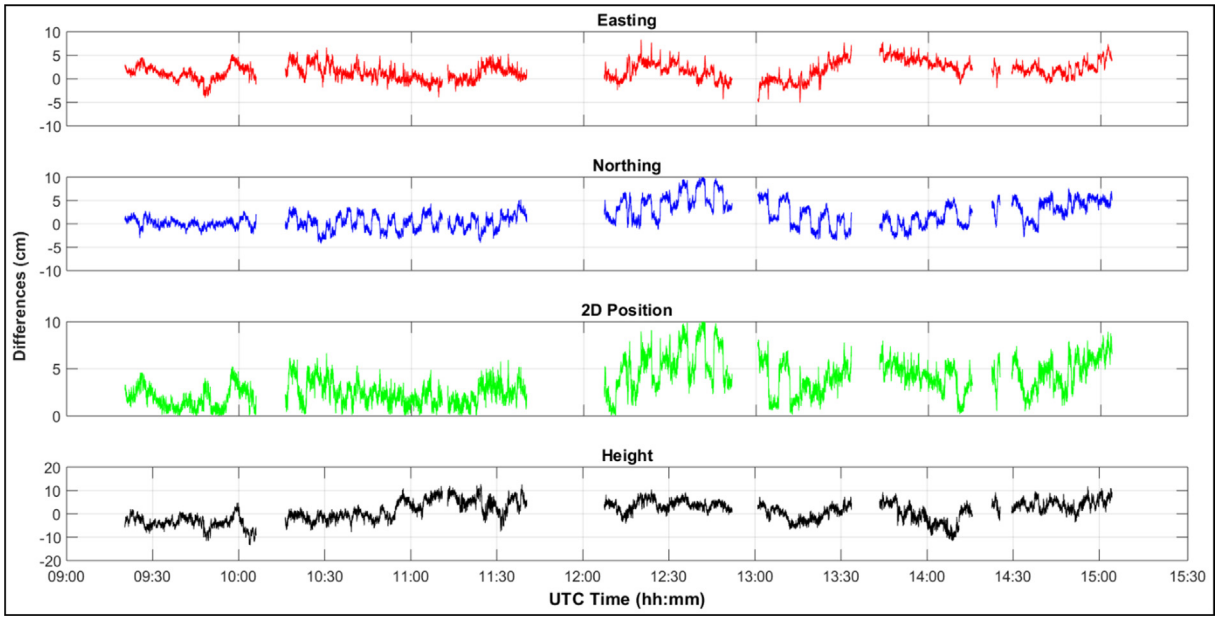

Fig. 5. Differences between known-coordinates and single-baseline RTK.

cm to +5 cm for both in easting and northing components and approximately −10 cm to +10 cm for height component.

In order to make an accurate analysis of the used methods, the *Root Mean Square Error* (*RMSE*) were calculated within the equations given below:

$$RMSE_{easting} = \pm\sqrt{\frac{1}{n}\sum_{i=1}^{n}\left(m_{easting_i} - k_{easting_i}\right)^2} \tag{21}$$

$$RMSE_{northing} = \pm\sqrt{\frac{1}{n}\sum_{i=1}^{n}\left(m_{northing_i} - k_{northing_i}\right)^2} \tag{22}$$

$$RMSE_{2D} = \pm\sqrt{RMSE_{easting}^2 + RMSE_{northing}^2} \tag{23}$$

$$RMSE_{height} = \pm\sqrt{\frac{1}{n}\sum_{i=1}^{n}\left(m_{height_i} - k_{height_i}\right)^2} \tag{24}$$

$$RMSE_{3D} = \pm\sqrt{RMSE_{easting}^2 + RMSE_{northing}^2 + RMSE_{height}^2} \tag{25}$$

where; $m_{easting_i}$, $m_{northing_i}$, and m_{height_i} are the easting, northing, and height components of the ith measurement epoch obtained from handled methods; $k_{easting_i}$, $k_{northing_i}$ and k_{height_i} are the corresponding known coordinates calculated from post-processed kinematic measurements; n is the number of measurement epoch; i is an integer ranging from 1 to n; $RMSE_{easting}$ is the *Root Mean Square Error* of easting component; $RMSE_{northing}$ represent the *Root Mean Square Error* of northing component; $RMSE_{2D}$ is the *Root Mean Square Error* of hor-

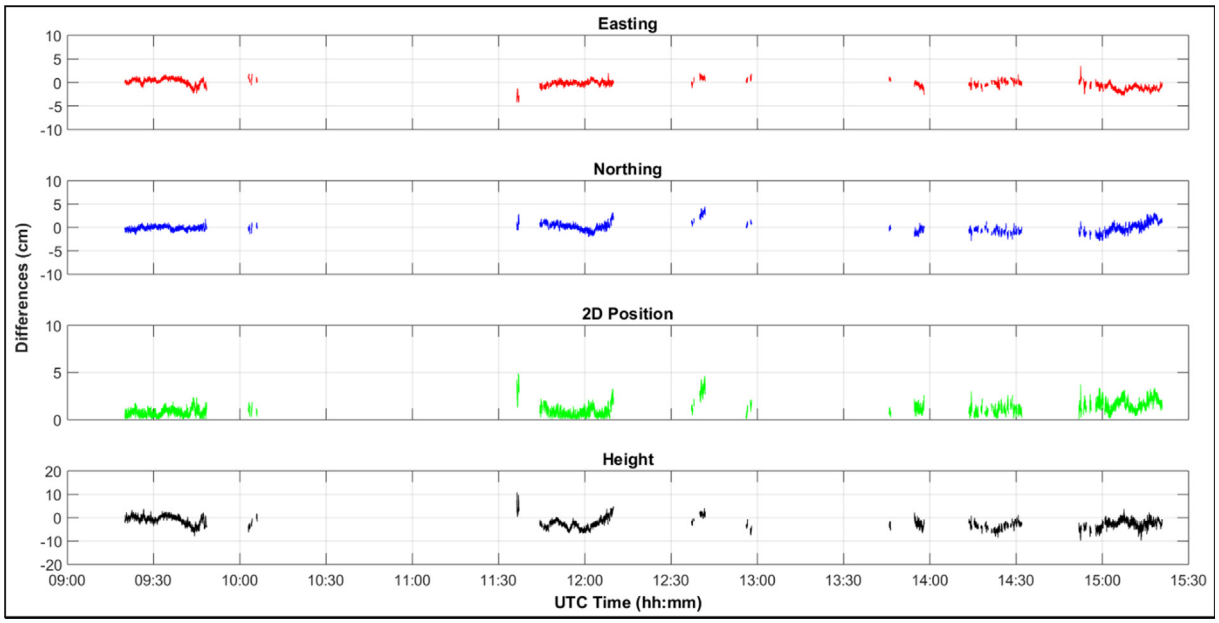

Fig. 6. Differences between known-coordinates and network RTK.

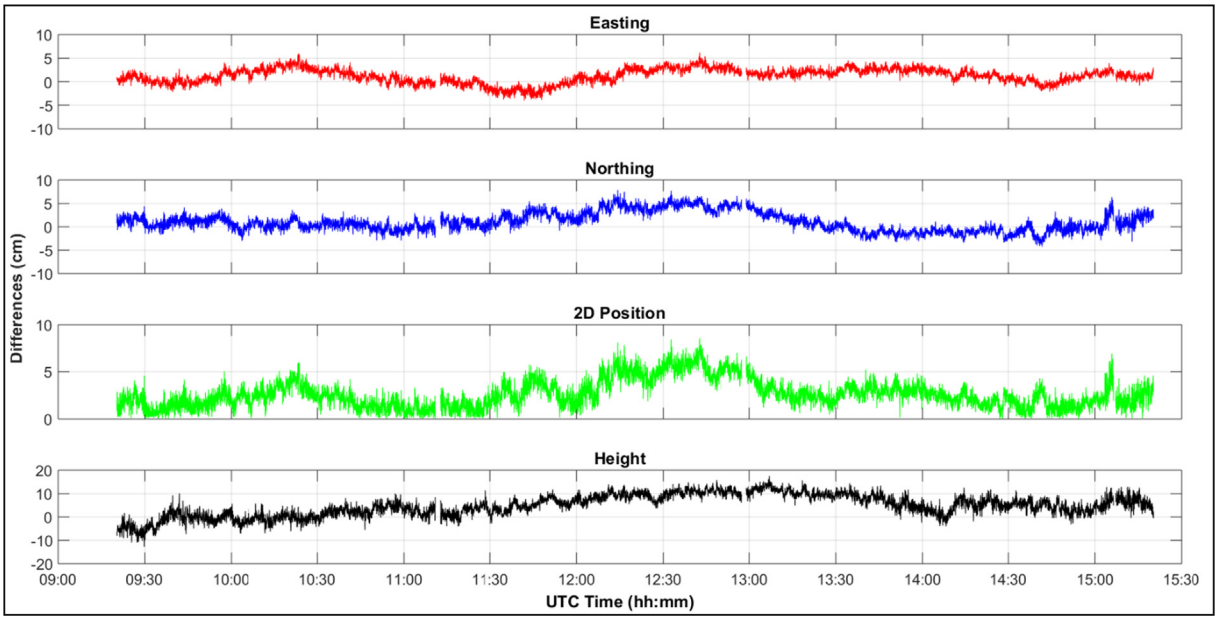

Fig. 7. Differences between known-coordinates and CenterPoint RTX.

izontal (2D) position, $RMSE_{height}$ is the *Root Mean Square Error* of ellipsoidal height component and $RMSE_{3D}$ *Root Mean Square Error* of 3D position.

The mean values of the differences for the easting, northing, 2D position, height components and 3D position with Root Mean Square Error (RMSE) are given in Table 1.

5. Results and discussion

The results obtained from the data processing are investigated in detail below.

Single-baseline RTK Results: According to Fig. 5 and Table 1, it is clearly seen that the mean values between Single-baseline RTK and relative solution were found 4 cm for the 2D position and 1 cm for height component. In terms of accuracy, the RMSE values were found ± 4 and ±5 cm for 2D position and height components, respectively. The results show that the 2D positioning can be conducted within a few centimetre-level of accuracy in most of the measurements.

However, when Fig. 5 was examined, 83.4% of the test measurements, which consisted of a total of 21,347 measuring epochs, were able to achieve a solution. For the remaining 16.6%, the cor-

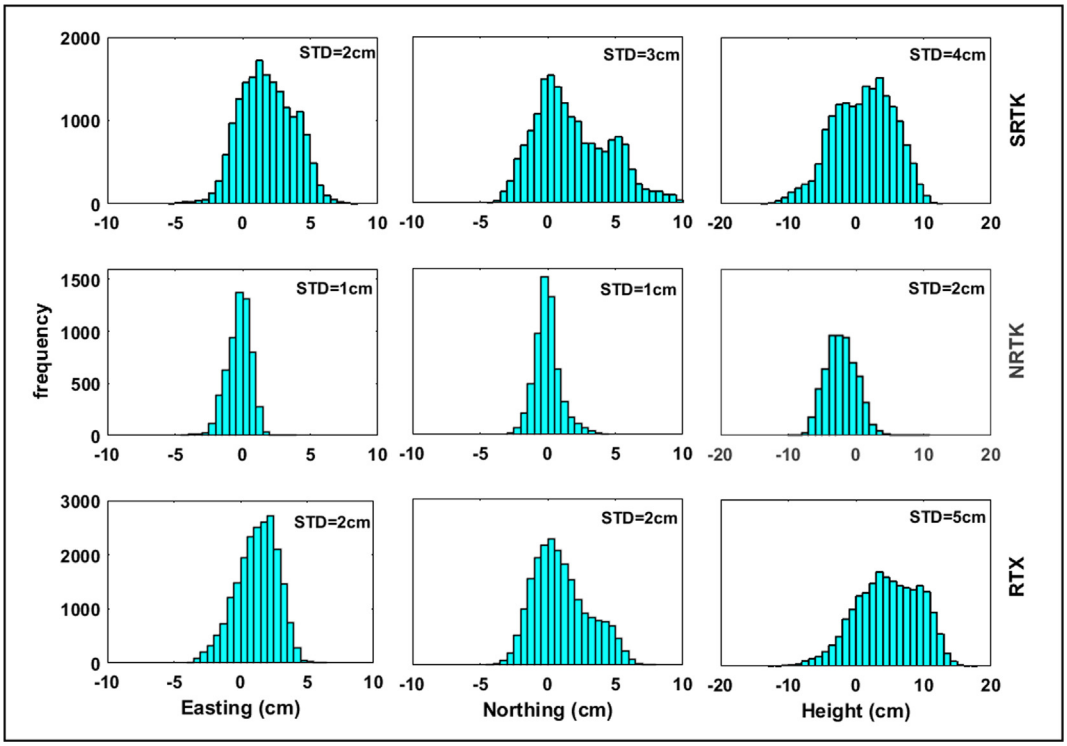

Fig. 8. Positioning differences distribution (*top: Single-baseline RTK, middle: Network RTK and bottom: Trimble CenterPoint RTX*).

Table 1
Mean and RMSE values for calculated differences.

Methods		Easting (cm)	Northing (cm)	2D pos. (cm)	Height (cm)	3D pos. (cm)
Single-baseline RTK	*mean*	2	2	4	1	6
	RMSE	±3	±3	±4	±5	±6
Network RTK	*mean*	0	0	1	−2	3
	RMSE	±1	±1	±1	±3	±3
CenterPoint RTX	*mean*	1	1	3	5	6
	RMSE	±2	±2	±3	±7	±7

rections could not be received, so the solution could not be obtained. This is due to the fact that the topographic structure of the study area did not allow the radio-link correction to be reached continuously from the reference station during all measurements. As it was mentioned before, there are hills covered by dense trees and deep valleys around the dam lake where the study was carried out.

Network RTK Results: As it is clearly seen from Fig. 6 and Table 1, the mean differences in 2D position were found 1 cm with ±1 cm RMSE and −2 cm as a mean value with ±3 cm RMSE in height for Network RTK-derived coordinates. These results reveal that the positioning could be conducted homogeneously with cm level of accuracy when providing the fix solution after a few second initialization time.

On the other hand, Fig. 6 shows that the position solution was achieved from only 28.5% of the measurements, which lasted for 6 h. It is seen that some part of the measurement area has no cellular coverage; therefore, it was not possible to access the internet and because of this, the corrections from TUSAGA-Aktif were not received during the measurements.

CenterPoint RTX Results: Fig. 7 and Table 1 show that the coordinate differences between RTX and the relative solutions have 3 cm mean and ±3 cm RMSE in horizontal component and 5 cm mean and ±7 cm RMSE in height component. The position accuracy of this study obtained with RTX RT-PPP technique is quite high compared to the above discussed studies using IGS-RTS (i.e.,Yang et al. [41]). Considering Fig. 7, it was seen that there was no problem with correction receiving from L-band geostationary satellite through the surveying unlike the Single-baseline and Network RTK methods.

In RTX technology, the cm-level high accurate positioning was possible using only one GNSS receiver without the need for a base station. Single-baseline or Network RTK requires the use of either a temporary or permanent base station. Furthermore, the accuracy performance of the RTK method is impacted by the distance between the rover and its base station. However, Trimble CenterPoint RTX can provide high accuracy positioning worldwide without the constraints of a local or Network RTK base station(s). In its current status, it offers an ideal solution in challenging field conditions where no networks are available or areas without the cellular coverage, thus without any internet access.

The attainable accuracies obtained from the handled methods are sufficient to meet the requirements for a majority of marine survey applications, including navigation, precise hydrographic surveying, attitude determination, ocean buoy positioning, cable and pipeline lying, dredging, crustal deformation monitoring, etc. Furthermore, the accuracies obtained from all used techniques can meet exceedingly the minimum positional accuracy requirement for several international hydrographic organization and authorities like Canadian Hydrographic Service (CHS), International Hydrographic Organization, (IHO), Land Information New Zealand (LINZ), United States Army Corps of Engineers (USACE), and Swedish Maritime Administration (SMA) for preparing nautical charts.

6. Conclusions

Improvements in technology have influenced almost everything in today's world and led to important developments. These developments have also a strong presence in the surveying discipline, and as a result, many new positioning methods and techniques have emerged in the surveying area. Many surveying applications requiring costly field and intensive office work a few decades ago have now become much easier, faster, more robust, and reliable.

In this study, the performance of Single-baseline RTK, Network RTK methods, and one of the RT-PPP positioning techniques, RTX Correction Service, were examined in a dynamic environment. Among all these methods, the Network RTK (TUSAGA-Aktif) provided more accurate results in terms of 2D position and height components. However, due to the cellular connection restriction in our study area, corrections could not be received for a significant part of the measurements (71.5%). Similarly, in Single-baseline RTK measurements, there were parts where positioning could not be performed due to a lack of correction (16.6% of all measurements). The results imply that the widely used RTK methods (Single-baseline and Network RTK) could be used in a dynamic environment for positioning as long as it can receive corrections. However, it should be pointed out that, these methods could not be used in some harsh terrain conditions that restrict or limit the radio connection or cellular coverage, and that these conditions can often be encountered especially in some marine environments such as narrow channels, ravines, canyons, straits, water mass that surrounded by high mountains/hills, dams situated in a deep valley covered by the dense trees, etc., where marine survey are made frequently.

When all the methods are examined in terms of availability, and ease of use, it was seen that the RTX RT-PPP method overcomes the other methods. The RTX reduced the surveying cost while requiring a few personnel and equipment besides it needs less time for pre-planning and logistics when compared to the requirements of conventional GNSS geodetic surveying methods. The overall results showed that the RTX provides homogenous, reliable, quick and seamless cm-level positioning while providing the productivity of RTK positioning using only a single GNSS receiver. Receiving the corrections from satellites will ensure that field surveying operations are performed in areas where there is no cellular network, without any interruption. In general, it can be said that any of the methods discussed in this study can be used easily in all marine applications that require accuracy of cm-dm.

Each of these methods has its prominent positive aspects and some disadvantages. The users have the flexibility to choose the proper method for them, taking into account the required accuracy, available field equipment, surveying budget, and environmental conditions of the study area. It can easily be said that all three methods handled in our study will produce similar results under normal terrain conditions; however, when the measurements are made in the harsh environment, the expected performance of the methods may not be obtained. From this point of view, the appropriate method and correction receiving type

(i.e., radio-modem, internet, cellular, satellite) are very crucial, and they should be selected by considering the field conditions.

CRediT authorship contribution statement

Reha Metin Alkan: Project administration, Funding acquisition, Conceptualization, Methodology, Writing - original draft, Writing - review & editing. **Serdar Erol:** Conceptualization, Methodology, Supervision, Software, Validation, Formal analysis, Investigation, Writing - review & editing, Visualization. **Veli İlçi:** Investigation, Resources, Visualization, Project administration. **İ. Murat Ozulu:** Investigation, Resources, Visualization.

Declaration of Competing Interest

The authors declare that they have no known competing financial interests or personal relationships that could have appeared to influence the work reported in this paper.

Acknowledgments

The authors would like to thank the CSY Engineering, Graftek Companies, Oğuzlar Municipality for organizing and providing full technical support for this study.

References

[1] R.M. Alkan, Cm-level high accurate point positioning with satellite-based GNSS correction service in dynamic applications, J. Spatial Sci. (2019), https://doi.org/10.1080/14498596.2019.1643795.
[2] R.M. Alkan, S. Erol, I.M. Ozulu, V. Ilci, Accuracy comparison of post-processed PPP and real-time absolute positioning techniques, Geomatics Natl. Hazards Risk 11 (1) (2020) 178–190.
[3] K. Anantakarn, B. Witchayangkoon, Accuracy assessment of L-band atlas GNSS system in Thailand, Int. Trans. J. Eng. Manage. Appl. Sci. Technol. 10 (1) (2019) 91–98.
[4] O.A. Aykut, E. Gülal, B. Akpinar, Performance of Single Base RTK GNSS Method versus Network RTK, Earth Sci. Res. J. 19 (2) (2015) 135–139.
[5] B. Bramanto, I. Gumilar, M. Taufik, I.M.D.A. Hermawan, Long-range Single Baseline RTK GNSS Positioning for Land Cadastral Survey Mapping, in: E3S Web of Conferences, vol. 94, 2019, pp.1–8, https://doi.org/10.1051/e3sconf/20199401022.
[6] M. Brandl, X. Chen, H. Landau, C. Rodriguez-Solano, U. Weinbach, Anatomy of a centimeter-level precise point positioning service, GPS World, 2019. Available at: https://www.gpsworld.com/anatomy-of-a-centimeter-level-precise-point-positioning-service (accessed 30 January 2020).
[7] J. Carballido, M. Pérez-Ruiz, L. Emmi, J. Agüera, Comparison of positional accuracy between RTK and RTX GNSS based on the autonomous agricultural vehicles under field conditions, Appl. Eng. Agric. 30 (3) (2014) 361–366.
[8] X. Chen, T. Allison, W. Cao, K. Ferguson, S. Grunig, V. Gomez, A. Kipka, J. Köhler, H. Landau, R. Leandro, G. Lu, R. Stolz, N. Talbot, Trimble RTX, an Innovative New Approach for Network RTK, in: Proceedings of the 24th International Technical Meeting of The Satellite Division of the Institute of Navigation (ION GNSS 2011), Portland, OR, USA, 20-23 September 2011, 2011, pp. 2214–2219.
[9] X. Chen, H. Landau, F. Zhang, M. Nitschke, M. Glocker, A. Kipka, U. Weinbach, D. Salazar, in: Towards a Precise Multi-GNSS Positioning System Enhanced for the Asia-Pacific Region, Springer, Berlin, Heidelberg, 2013, pp. 277–290.
[10] P. Dabove, The usability of GNSS mass-market receivers for cadastral surveys considering RTK and NRTK techniques, Geod. Geodyn. 10 (4) (2019) 282–289.
[11] P. Denys, C. Pearson, 2016. Positioning in Active Deformation Zones-implications for NetworkRTK and GNSS Processing Engines. FIG Article of the Month-March 2016. http://www.fig.net/resources/monthly_articles/2016/denys_pearson_march_2016.asp (accessed 30 January 2020).
[12] P. Denys, A. Liggett, R. Odolinski, C. Pearson, D. Stewart, R. Winefield, Network RTK-New Zealand, A Summary of the Concepts, Methods, Limitations and Services in New Zealand. NZIS Positioning and Measurement, 2017, pp. 41. Available at https://www.surveyspatialnz.org/Attachment?Action=Download&Attachment_id=3121 (accessed 30 January 2020).
[13] A.F. dos Santos, R.P. da Silva, C. Zerbato, P.C. de Menezes, E.H. Kazama, C.S.S. Paixão, M.A. Voltarelli, Use of real-time extend GNSS for planting and inverting peanuts, Precis. Agric. 20 (4) (2018) 1–17, https://doi.org/10.1007/s11119-018-9616-z.
[14] K. Doucet, M. Herwig, A. Kipka, P. Kreikenboh, H. Landau, R. Leandro, M. Moessmer, C. Pagels. Introducing ambiguity resolution in web-hosted global multi-GNSS precise positioning with trimble RTX-PP, in: Proceedings of the 25th International Technical Meeting of The Satellite Division of the Institute of Navigation (ION GNSS 2012), Nashville, Tennessee, USA, 17–21 September, 2012, , 2012, pp.1115–1125.
[15] A. El-Mowafy, Precise real-time positioning using network RTK, in: Shuanggen Jin (Ed.), Global Navigation Satellite Systems: Signal, Theory and Applications, InTech Publishing, 2012, pp. 161–188.
[16] M. Elsobeiey, S. Al-Harbi, Performance of real-time precise point positioning using IGS real-time service, GPS Solut. 20 (3) (2016) 565–571.
[17] M.J. Garbor, R.S. Nerem, Satellite-satellite single difference phase bias calibration as applied to ambiguity resolution, J. Inst. Navigat. 49 (4) (2002) 223–242.
[18] M. Glocker, H. Landau, R. Leandro, M. Nitschke, Global precise multi-GNSS positioning with trimble CenterPoint RTX, in: Proceedings of 6th ESA Workshop on Satellite Navigation Technologies (NAVITEC 2012) & European Workshop on GNSS Signals and Signal Processing. Noordwijk, Netherlands, 5-7 December, 2012, 2012, pp. 1–8.
[19] T. Grinter, Precise Point Positioning-The Evolution of an Alternative GNSS Positioning Solution Master of Engineering Thesis, University of New South Wales, Sydney, Australia, 2018, p. 138.
[20] I. Gumilar, B. Bramanto, F.F. Rahman, I.M.D.A. Hermawan, Variability and Performance of Short to Long-Range Single Baseline RTK GNSS Positioning in Indonesia. E3S Web of Conferences, vol. 94, 2019, pp.1–5. https://doi.org/10.1051/e3sconf/20199401012.
[21] B. Hofmann-Wellenhof, K. Legat, M. Wieser, Navigation: Principles of Positioning and Guidance, first ed., Springer, Vienna-New York, 2003.
[22] B. Hofmann-Wellenhof, H. Lichtenegger, E. Wasle, GNSS-Global Navigation Satellite Systems: GPS, GLONASS, Galileo, and More, Springer-Verlag, Vienna, Austria, 2008.
[23] J.J. Hutton, N. Gopaul, X. Zhang, J. Wang, V. Menon, D. Rieck, A. Kipka, F. Pastor, Centimeter-level, Robust GNSS-Aided Inertial Post-processing for Mobile Mapping without Local Reference Stations, The International Archives of the Photogrammetry, Remote Sensing and Spatial Information Sciences, Volume XLI-B3, 2016 XXIII ISPRS Congress, 12-19 July 2016, Prague, Czech Republic, 2016.
[24] V. Ilci, Accuracy comparison of real-time GNSS positioning solutions: case study of mid-north Anatolia, Measurement 142 (2019) 40–47.
[25] R. Leandro, H. Landau, M. Nitschke, M. Glocker, S. Seeger, X. Chen, A. Deking, M. BenTahar, F. Zhang, K. Ferguson, R. Stolz, N. Talbot, G. Lu, T. Allison, M. Brandl, V. Gomez, W. Cao, A. Kipka, RTX positioning: the next generation of cm-accurate real-time GNSS positioning, in: Proceedings of the 24th International Technical Meeting of the Satellite Division of the Institute of Navigation (ION GNSS 2011), Portland, Oregon, USA, 19-23 September 2011, 2011, pp. 1460–1475.
[26] R. Leandro, H. Landau, M. Nitschke, M. Glocker, S. Seeger, X. Chen, A. Deking, M. Ben Tahar, F. Zhang, K. Ferguson, R. Stolz, N. Talbot, G. Lu, T. Allison, M. Brandl, V. Gomez, W. Cao, A. Kipka, Real-Time Extended GNSS Positioning: A New Generation of Centimeter-Accurate Networks, GPS World, 2012. Available at: https://www.gpsworld.com/machine-control-agprecision-agreal-time-extended-gnss-positioning-13177 (accessed 30 January 2020).
[27] L.A. Lipatnikov, S.O. Shevchuk, 2019. Cost Effective Precise Positioning with GNSS. The International Federation of Surveyors (FIG), Denmark, March 2019, pp. 82. Available at: https://www.fig.net/resources/publications/figpub/pub74/Figpub74.pdf (accessed 30 January 2020).
[28] C.R. McHugh, I. Church, M. Kim, D. Maggio, Comparison of horizontal and vertical resolvable resolution between repetitive multi-beam surveys using different kinematic GNSS methods, Int. Hydrograph. Rev. 14 (2015) 7–18.
[29] J.F.G. Monico, H.A. Marques, Í. Tsuchiya, R.T. Oyama, W.R.S. Queiroz, M.C. Souza, J.P. Wentz, Real time PPP applied to airplane fligtht tests, Boletim de Ciências Geodésicas 25 (2) (2019).
[30] A. Nardo, R. Drescher, M. Brandl, X. Chen, H. Landau, C. Rodriguez-Solano, S. Seeger, U. Weinbach, Experiences with trimble CenterPoint RTX with fast convergence, European Navigation Conference 2015, Bordeaux, France, 7–10 April 2015, 2015.
[31] Z. Nie, F. Liu, Y. Gao, Real-time precise point positioning with a low-cost dual-frequency GNSS device, GPS Solut. 24 (1) (2020) Article:9.
[32] A. Ochałek, W. Niewiem, E. Puniac, P. Ćwiąkała, Accuracy evaluation of real-time GNSS precision positioning with RTX trimble technology, Civil Environ. Eng. Rep. 28 (4) (2018) 49–61.
[33] D. Odijk, L. Wanninger, Differential positioning, in: Peter J.G. Teunissen, Oliver Montenbruck (Eds.), Springer Handbook of Global Navigation Satellite Systems, Springer International Publishing AG, Switzerland, 2017, pp. 753–780.
[34] S. Ogutcu, I. Kalaycı, Investigation of network-based RTK techniques: a case study in urban area, Arab. J. Geosci. 9 (3) (2016) 1–12.
[35] D. Prochniewicz, R. Szpunar, J. Walo, A new study of describing the reliability of GNSS network RTK positioning with the use of quality indicators, Meas. Sci. Technol. 28 (1) (2017).
[36] M. Richter, Using PPP corrections in precise real-time applications, GIM Int. 6 (33) (2019) 32–33.
[37] N. Talbot, X. Chen, N. Reussner, M. Brandl, M. Nitschke, C. Rodriguez-Solano, F. Zhang, Trimble RTX orbit determination and user positioning performance with beidou satellites, in: International Global Navigation Satellite Systems Conference (IGNSS 2016), Sydney, Australia, 6–8 December 2016, 2016.
[38] L. Wanninger, Introduction to Network RTK. IAG Working Group 4.5.1: Network RTK, 11 December 2006, 2006.

[39] G. Wübbena, A. Bagge M. Schmitz, Network Based Techniques for RTK Applications, in: Proceedings of GPS Symposium 2001, Japan Inst. of Navigation, Tokyo, Japan, Nov. 14–16, 2001, 2001, pp. 53–65.
[40] Y. Xu, W. Chen, Performance analysis of GPS/BDS dual/triple-frequency network RTK in urban areas: a case study in Hong Kong, Sensors 18 (8) (2018).
[41] F. Yang, L. Zhao, L. Li, S. Feng, J. Cheng, Performance evaluation of kinematic BDS/GNSS real-time precise point positioning for maritime positioning, J. Navigat. 72 (1) (2019) 34–52.
[42] J. Yu, B. Yan, X. Meng, X. Shao, H. Ye, Measurement of bridge dynamic responses using network-based real-time kinematic GNSS technique, J. Surv. Eng. 142 (3) (2016).
[43] URL 1, IGS Real-time Service. Available at: http://www.igs.org/rts (accessed 30 January 2020).
[44] URL 2, Trimble CenterPoint RTX. Available at: https://www.trimble.com/Positioning-Services/CenterPoint-RTX.aspx (accessed 30 January 2020).
[45] URL 3, Trimble R10 Integrated GNSS System. Available at: https://geospatial.trimble.com/products-and-solutions/r10#product-support (accessed 30 January 2020).
[46] URL 4: GrafNav/GrafNet User Manual. Available from: https://www.novatel.com/assets/Documents/Waypoint/Downloads/GrafNav-GrafNet-User-Manual-870.pdf (accessed 30 January 2020).